

# Biodegradable Composite Materials Based on Cassava Starch and Reinforced with Topinambur (*Helianthus tuberosus*) Aerial Part Fiber

Luisa Fernanda Sierra Montes<sup>1,2</sup>, Mariana Andrea Melaj<sup>3,4</sup>, María Cecilia Lorenzo<sup>5,6</sup>, Laura Ribba<sup>7,8,\*</sup> and María Alejandra García<sup>1,2,\*</sup>

<sup>1</sup> CIDCA-UNLP-CONICET-CICPBA, 47 y 116, La Plata B1900AJJ, Argentina; luisaf.2294@gmail.com (L.F.S.M.)

<sup>2</sup> Facultad de Ciencias Exactas, UNLP, 47 y 115, La Plata B1900AJJ, Argentina

<sup>3</sup> Facultad de Ingeniería, Universidad de Buenos Aires, Buenos Aires 1063, Argentina; mmelaj@fi.uba.ar (M.A.M.)

<sup>4</sup> Instituto de Tecnología en Polímeros y Nanotecnología (ITPN), CONICET – Universidad de Buenos Aires, Buenos Aires C1127AAR, Argentina

<sup>5</sup> INTI–Materiales Avanzados, Av. Gral. Paz 5445, San Martín, Buenos Aires B1650WAB, Argentina; clorenzo@inti.gov.ar (M.C.L.)

<sup>6</sup> Instituto de Investigación e Ingeniería Ambiental (3iA), UNSAM, San Martín, Buenos Aires B1650WAB, Argentina

<sup>7</sup> Departamento de Física, Facultad de Ciencias Exactas y Naturales, UBA, Buenos Aires C1428EGA, Argentina

<sup>8</sup> INTI, CONICET, Dirección de Materiales Avanzados, Áreas del Conocimiento, San Martín, Buenos Aires B1650WAB, Argentina

\* Corresponding author. E-mail: lribba@inti.gob.ar (L.R.); magarcia@quimica.unlp.edu.ar (M.A.G.)

Received: 9 February 2024; Accepted: 15 April 2024; Available online: 18 April 2024

**ABSTRACT:** The cultivation of topinambur (*Helianthus tuberosus*) has aroused the interest of producers since it is a source of inulin and can be used for biofuel production. During tuber processing, the aerial part of the crop remains as a by-product with no practical application. This work aimed to characterize the fibers obtained from the aerial part of topinambur and to evaluate their reinforcing potential in cassava starch-based films. Starch-based films with topinambur fiber (0, 5, and 10%) were prepared by extrusion followed by thermocompression. Topinambur residue contains 88.6% of total fiber, 8.5% ash, and 0.68% lipid. Mechanical film properties evidenced the reinforcement action of topinambur fiber, 10% content was able to increase up to 70% the Young's modulus. SEM micrographs evidenced the good fiber-matrix interaction. UV-visible capacity, opacity, and chromaticity parameters of TPS films increased with fiber content in the formulation. Fiber incorporation improved the hydrophobicity of the biocomposite materials by increasing the contact angle. Starch-based films biodegraded more than 55% after 110 days, showing a similar trend to that of microcrystalline cellulose. Thus, topinambur residue can be effectively used as a reinforcing agent for TPS materials, being an innovative and non-toxic additive within the circular economy premises.

**Keywords:** Biodegradable materials; Thermoplastic starch; Reinforcing agent; Topinambur residue; Agriculture



© 2024 by the authors; licensee SCIEPublish, SCISCAN co. Ltd. This article is an open access article distributed under the CC BY license (<http://creativecommons.org/licenses/by/4.0/>).

## 1. Introduction

Currently, one of the most prominent global environmental problems is pollution from the extended use of plastics from fossil fuels [1]. Global plastics production reached 368 million metric tons (Mt) in 2019 and is expected to double over the next 20 years [2]. Although the use of plastic in agriculture is fairly low compared to the general use of plastic (only 3% of plastics produced in Europe are used in agriculture); agricultural plastics are made of polyethylene, which is not biodegradable and must be removed after use. Besides, their recovery is generally deficient due to the embrittlement and fragmentation effect of radiation, resulting in their accumulation in agricultural soils and watercourses [3].

A promising approach to reduce pollution associated with the utilization of plastics is the use of biodegradable polymeric matrices. Starch offers several advantages as being low cost, abundant, renewable, and biodegradable, in addition

to the fact that it can be processed by conventional industrial techniques such as extrusion, injection, and compression molding. Nevertheless, poor mechanical and water barrier properties have limited its application [4–6].

An alternative to overcome these disadvantages is the addition of inorganic or organic fillers. Compared to inorganic fillers, lignocellulosic materials are being extensively studied due to their renewable and biodegradable nature, low cost and density, as well as their inherent flexibility and safety, which make them easy to process [7,8]. This versatility and local availability has contributed to a growing preference in recent years for natural fibers over synthetic fibers such as glass fiber [9]. Lignocellulosic materials have a chemical structure compatible with starch, a factor that promotes good interfacial adhesion between the matrix and the filler. Recent studies developed composite materials with superior properties employing different fillers, such as blueberry pomace [10], agave fibers [11], banana inflorescence waste fiber [5], pineapple leaf fiber [12], sugar palm fibers [13] and oil palm mesocarp fiber [14].

Likewise, Maraveas [15] has exhaustively revised the production of sustainable and biodegradable polymers from agricultural waste, with special emphasis on fiber-reinforced composite materials.

Topinambur (*Helianthus tuberosus*) is a plant native to North America, which can grow and adapt to different environmental conditions with minimal fertilizer, pesticide, and water requirements, determining factors in its worldwide expansion. This herbaceous plant with branched stems can reach up to 3 m in height and produces tubers traditionally used in the production of fodder and horticulture. Topinambur tubers are a source of inulin and fructooligosaccharides, which have nutritional and functional properties suitable for diabetics and celiacs; besides the interest as raw material for the production of bioethanol [16,17]. After processing the tuber, the aerial part of the crop is left as a remnant, a residue that could be valorized as a reinforcement of biodegradable materials.

The removal of the amorphous layer of lignin and hemicellulose on the fibers is a strategy used to increase surface roughness and the amount of partially exposed crystalline cellulose; in order to obtain a stronger compatibility between the fibers and starch. However, this modification requires high energy and chemical treatments that are harmful to health and the environment [14]. Therefore, in this work, we propose the integral utilization of the fiber as a potential reinforcement for starch-based films.

In this work the natural wastes obtained from the production of topinambur tubers are fully characterized for the first time. Moreover, their potential use as a reinforcement in thermoplastic cassava starch (TPS) films is explored, which, to our knowledge, has not been reported in any study to date. This application not only adds value to the residue but also improves the performance of starch-based bioplastics and produces a material that could potentially be transformed into seedling pots or other agroecological products to replace non-biodegradable synthetic plastics.

## 2. Materials and Methods

### 2.1. Materials

Cassava starch was provided by Aldema Cooperative (Misiones, Argentina) and residues of the aerial part of the topinambur crop (stems) were provided by the Faculty of Agronomy (UNLP) of La Plata City (Buenos Aires, Argentina). Once received, the stems of topinambur crop were grounded into powder in a high-speed multifunction grinder (Damai HC-250Y, Zhejiang, China) and later sieved with a 500  $\mu\text{m}$  mesh, in order to have a limited maximum particle size. Topinambur fiber was stored in airtight flasks until used. Analytical grade glycerol and sorbitol (Anedra, Buenos Aires, Argentina) were used as plasticizers.

### 2.2. Topinambur Residue Characterization

The filler particle size distribution was determined using a sieve tower (ALEIN international, Buenos Aires, Argentina) with the following set of standard mesh sizes: 500, 425, 300, 250, 180, 150, 75, and 53  $\mu\text{m}$ , as was described by Versino and Garcia [18]. The morphology and surface appearance of the sieved fibrous residue were examined by SEM Phenom ProX (Atlanta, GA, USA); the samples were coated with a thin layer of platinum and were analyzed using an acceleration voltage of 5 kV in high vacuum mode.

Residual moisture content was quantified gravimetrically by placing the samples in an oven (GMX 9203A PEET LAB, USA) at 105  $^{\circ}\text{C}$  until constant weight. Ash was also determined using the AOAC 923.03 gravimetric method [19], the samples were incinerated in a muffle (Indef 331, Córdoba, Argentina). The determination of total lipids was studied using

the Soxhlet extraction method with hexane. Fibrous residue samples were analyzed by Kjeldahl method according to AOAC 984.13 for protein content [20]. Total dietary fiber was determined by the AOAC 985.29 enzymatic-gravimetric method [21], using the Total Dietary Fiber Assay Kit K-TDFR 05/12 (Megazyme®, Bray, Ireland). Lignin content was determined with the Klason method following the TAPPI T222 om-02 (2011) [22]. The cellulose and hemicellulose content was determined by the acid detergent fiber (ADF) and neutral detergent fiber (NDF) methods, according to modifications realized by Strack, García, Cabezas, Viña and Dini [23]. All experiments were performed at least in duplicate and were expressed as percentage (%) on a dry basis.

The thermal stability of the topinambur fiber residue and cassava starch was determined using a TA Instruments Q-500 (Delaware, USA) thermo-balance, the samples were heated from 30 °C to 800 °C at a heating rate of 10 °C/min in a nitrogen atmosphere (flow rate 60 mL/min). Considering that total dehydration is achieved at 105 °C, the percentage of retained water ( $W_{\%}$ ) was calculated as:

$$W_{\%} = (m(T) - m_{105^{\circ}\text{C}}) * \left( \frac{100}{(m_{\text{initial}} - m_{105^{\circ}\text{C}})} \right) \quad (1)$$

where,  $m(T)$  is the mass at temperature ( $T$ ),  $m_{105^{\circ}\text{C}}$  is the mass at 105 °C and  $m_{\text{initial}}$  is the initial mass of the sample.

Fourier Transformed Infrared (FTIR) spectra were obtained on a Nicolet iS10 Thermo Scientific Analyzer (Madison, USA) equipped with Attenuated Total Reflectance (ATR). Spectra were analyzed in the range of 4000 to 400  $\text{cm}^{-1}$  as an average of 32 scans with a resolution of 4  $\text{cm}^{-1}$ .

### 2.3. Preparation of the Biocomposite Films

Mixtures of cassava starch, topinambur residue, plasticizers and water were prepared. The added fiber contents varied between 0 and 20% w/w starch base, however it was observed that contents greater than 10% w/w starch base induced defects in the TPS matrix, for this reason the topinambur fiber content was limited to 10% w/w starch base. Likewise, based on preliminary assays, the concentration and type of plasticizers used were selected in order to improve the processability of the mixtures by extrusion and the subsequent obtaining of the materials by thermocompression. Thus, mixtures of cassava starch, glycerol, sorbitol, distilled water (70:10:10:10% w/w), and topinambur residues (0, 5, and 10% w/w starch base) were prepared. The films were designated TPS for the control, TPS-topi5 for the addition of 5% fiber, and TPS-topi10 for the one containing 10% fiber. The systems were processed in a Brabender OHG (Duisburg, Germany) extruder, in the single screw module using a barrel temperature profile from the feed section to the metering section of 85, 100, 110, 115, 125 °C, and 70 rpm. Finally, the films were prepared by compression molding in a hydraulic press (Smaniotto, Buenos Aires, Argentina). The composite mixture was preheated at 130 °C for 2 min and compressed at 130 °C for 5 min at 40 bar, 5 min at 110 bar, and 5 min at 160 bar. Pressing conditions were selected based on preliminary optimization experiments. The films were cooled under refrigeration pressure for approximately 10 min and then removed from the molds.

### 2.4. Films Characterization

Before characterization, films were conditioned at 25 °C and 60% RH. Film thickness was measured using a digital ultrasonic thickness gauge meter CM-8822 (REED Instruments, NY, USA), on a non-ferrous surface for non-conductive materials. At least ten measurements on each sample were taken and the mean value was informed. The material's density ( $\text{g}/\text{cm}^3$ ) was determined gravimetrically employing a precision balance with an accuracy of 0.1 mg on 2 cm × 2 cm samples of known thickness. According to Monroy et al. [24]. These measurements were performed in quintupled.

The cryo-fracture surfaces of the films were observed under the SEM microscope Phenom ProX (Atlanta, GA, USA), using a 5 kV accelerating voltage, in high vacuum mode. The opacity and UV-visible barrier capacity were analyzed in a Hitachi U1900 spectrophotometer (Hitachi, Japan), to evaluate the barrier capacity of the film according to the Standard Test Method for Haze and Luminous Transmittance of Transparent Plastic Recommendations ASTM D1003-00 [25]. Color was measured with a Konica CR400 colorimeter (Osaka, Japan) using the CIELab scale: luminosity (L) and chromatic parameters  $a^*$  (red-green) and  $b^*$  (yellow-blue), color assays were performed in at least ten random positions by placing the film over the standard plate.

Tensile tests of the biocomposite films were evaluated by performing quasi-static tests in uniaxial conditions using a Universal Machine Instron model 5569 (Massachusetts, USA), in accordance with the ASTM D882 standard [26], a

minimum of ten probes of  $10 \times 100$  mm were assayed for each film formulation. The puncture tests were performed in a TA.XT2i texturometer—Stable Micro Systems (Surrey, UK) using a 3 mm diameter cylindrical probe (P3) at a deformation rate of 1 mm/s, the maximum force at rupture, the strain at rupture and the area under the curve (N mm) associated with the energy required to perforate the material were calculated, at least ten replicates were analyzed. Reported values correspond to the mean values of each mechanical parameter.

Moisture content of the films was determined gravimetrically by measuring the weight loss of the films after drying in an oven at 105 °C to constant weight, the values reported are the mean of at least three determinations. To study the surface wettability of the films, the contact angle was evaluated in a model 190 goniometer (Ramé-Hart, Instrument Co., NJ, USA). A drop of Milli-Q water grade was released onto different regions of the film surface and the contact angle was calculated from a digital image taken as soon the drop reached the sample, at least ten replicates were made for each film sample. The water absorption capacity of the films was quantified gravimetrically in a container at 100% relative humidity and 20 °C, the films were previously dried to constant weight in an atmosphere of anhydrous  $\text{CaCl}_2$ , the weight gain was recorded as a function of time, and the data were fitted to the mathematical model proposed by Elizalde, Pilosof and Bartholomai [27],

$$q = \frac{(Q * t)}{(B + t)} \quad (2)$$

where,  $q$  and  $Q$  are the water absorbed at time ( $t$ ) and at equilibrium respectively and  $B$  is the time required for samples to gain half of the equilibrium value ( $Q/2$ ). At least three replicates were analyzed for each sample.

The biodegradation test of the films was performed in soil according to the ISO 17556:2019 standard [28] by means of a respirometric test using an OxiTop-C (WTW, Weilheim, Germany). Microcrystalline cellulose (MCC) (Biopack, Buenos Aires, Argentina), was included as reference. The total organic carbon was measured in a LECO C744 carbon analyzer (California, USA) to estimate the theoretical  $\text{CO}_2$  demand ( $\text{ThCO}_2$ ) and subsequently the percentage of biodegradation as was described by Díaz-Díaz et al. [29]. In order to evaluate the toxicity of the residual soil, ecotoxicity tests were performed on the residues remaining from the biodegradation test according to the OECD 208 standard [30] evaluating the germination of tomato (*Solanum lycopersicum*) seeds. The parameters determined were the number of plants emerged, the maximum number of leaves per plant (Nmax leaves/plant), the plant height (cm) and the fresh weight (g).

## 2.5. Statistical Analysis

Statistical analysis of the results obtained was performed using the InfoStat software version 2020. Analysis of variance (ANOVA) was used to compare the mean differences between samples, with Fisher's Least Significant Difference (LSD) test at a significance level of  $\alpha = 0.05$ . Data were expressed as mean  $\pm$  standard deviations.

## 3. Results and Discussion

### 3.1. Characteristics of Topinambur Fiber

The chemical composition and morphology of topinambur fibers were initially characterized, as they determine the effects on the properties of the starch films. SEM micrographs show that topinambur fiber contains two types of particles, short fibers and particles without a defined shape (Figure 1a). These fibers also presented rough surfaces (Figure 1b). The chemical composition is presented in Table 1, and revealed a high content of organic material with 87.3% content of lignocellulosic fiber ( $(41.40 \pm 0.2)\%$  cellulose,  $(14.2 \pm 0.9)\%$  hemicellulose and  $(24.1 \pm 0.2)\%$  lignin), and 8.5% associated with minerals.

Comparable values were reported by Kar and Saikia [31] for *Calamus tenuis* cane fibers, with  $(37.4 \pm 1.4)\%$  cellulose,  $(31 \pm 1)\%$  hemicellulose, and  $(28.4 \pm 0.8)\%$  lignin. Cellulose is one of the major structural components that increases the mechanical strength, stability, and toughness of natural fibers [31], which is beneficial to the reinforcement of the composite material; in the case of topinambur fiber, it was the main structural component. The hemicellulose content of topinambur fiber was lower compared to *Calamus tenuis* cane fiber, high values can disintegrate the microfibrils cellulose, resulting in lower fiber strength [31]. Lignin acts against microbial attack and provides greater stiffness, but the mechanical properties are lower than those provided by cellulose [32]. Figure 1c shows the particle size distribution obtained using a sieve tower. A heterogeneous distribution was observed, with 11% of the particles larger than 53  $\mu\text{m}$ , and a higher contribution of larger particles (mainly 462  $\mu\text{m}$ ), which can be considered as a micrometric reinforcement.

**Table 1.** Chemical composition (% w/w) of aerial residue from the topinambur aerial part.

Total Dietary Fiber	Fiber			Humidity	Lipids	Protein	Ashes
	Klason Lignin	Cellulose	Hemicellulose				
87.3 ± 0.5	24.1 ± 0.2	41.4 ± 0.2	14 ± 1	8.9 ± 0.2	0.7 ± 0.2	1.33 ± 0.01	8.5 ± 0.2

**Note:** Reported values correspond to the mean ± standard deviation. Expressed on dry basis.

**Figure 1.** Topinambur residue characterization, scanning electron (SEM) micrographs at (a) 250× (b) 530× and (c) particle size distribution.

It was necessary to investigate the thermal stability of both topinambur fiber residue and cassava starch, in order to understand their behavior during extrusion processing. Thermogravimetric analysis (TGA) of topinambur residue and cassava starch (Figure 2a) present three stages of weight loss. The first, between 50–105 °C, is attributed to water evaporation or dehydration and shows that starch contains a higher amount of water of hydration compared to topinambur fiber. Figure 2d shows the percentage of retained water ( $W\%$ ), topinambur fiber is observed to have its water of hydration more weakly bound, and therefore loses water more easily compared to starch. Thus, starch has a greater amount of water of hydration (Figure 2a), which is more strongly bound, making its removal more expensive (Figure 2d). In addition, the moisture content in topinambur fibers corresponds to that previously mentioned in Table 1.

Figure 2b shows the percentage of weight loss on a dry basis. Here the second degradation zone of topinambur fiber can be seen from 210 to 350 °C, which is related to the degradation of organic compounds such as hemicellulose and cellulose [5]. On the other hand, cassava starch is more thermally stable since it starts its degradation at a higher temperature (250 to 350 °C) than topinambur fiber (Figure 2b). In this stage the complete breakdown of starch chains takes place [33]. Finally, the last thermal degradation zone happens after 400 °C. In topinambur fiber it is attributed to the phenolic compounds, part of the lignin cell wall [5]; meanwhile, for starch it can be related to the oxidation of partially decomposed starch [33]. The TGA curve (Figure 2b) shows a higher residual ash content for the topinambur fiber than for the starch, 20 and 10%, respectively, corresponding to the residual organic and inorganic matter in an inert atmosphere.

The derivative curve (Figure 2c) indicates that the degradation peak of starch is narrower with respect to that of topinambur fiber, suggesting that the fiber has certain heterogeneity in its composition as shown in Table 1. Figure 2c shows a small shoulder for starch near 300 °C, corresponding to the change in the slope of the weight loss at this temperature observed in Figure 2a. That could be attributed to a bimodal distribution of starch molecular weight due to late harvesting, as found by Sriroth et al. [34]. Taking into account the results of thermal characterization, it is clear that topinambur fiber is thermally stable and will not degrade during extrusion processing with the starch.

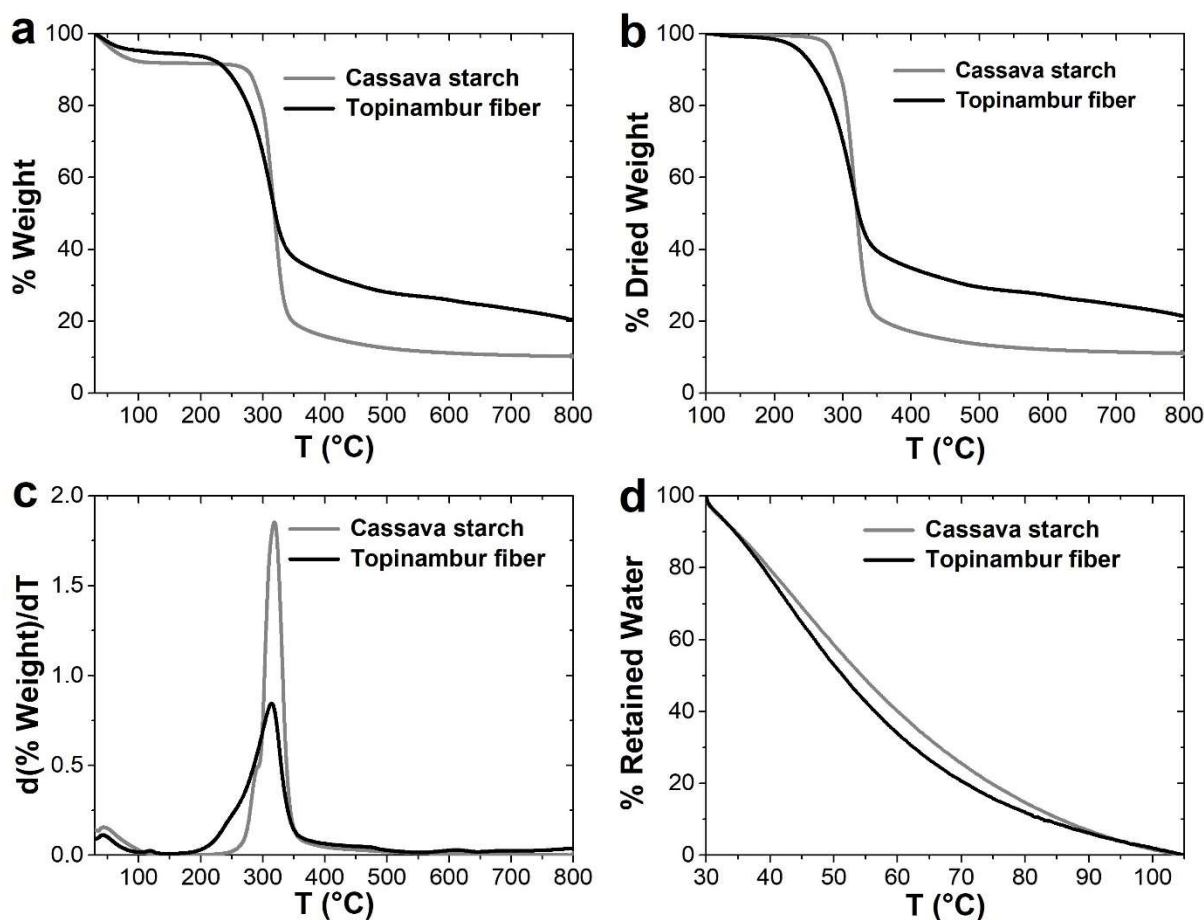
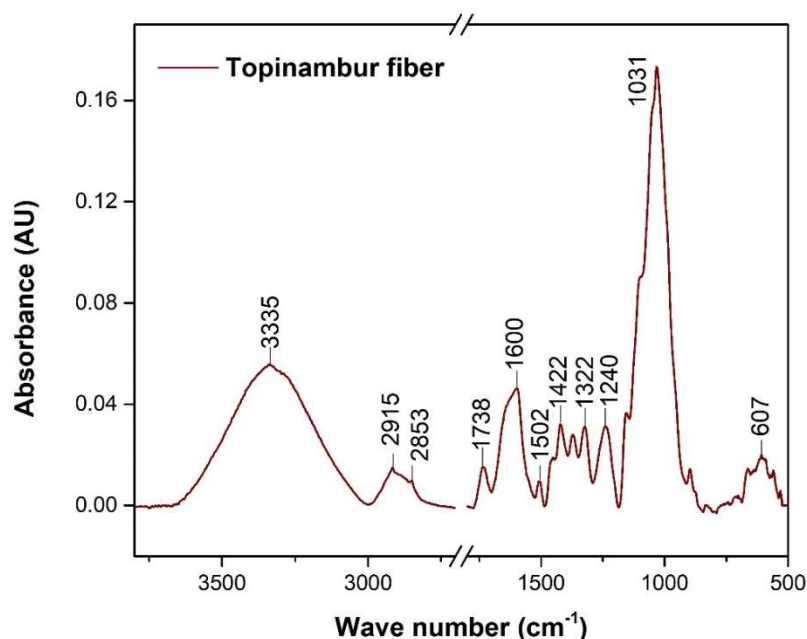


**Figure 2.** Thermogravimetric analysis (TGA) of topinambur fiber and cassava starch (a) percentage of mass loss, (b) percentage loss of mass in dried weight (c) derivative of mass loss, and (d) percentage of retained water.

The FTIR spectrum of topinambur fiber (Figure 3) shows the typical characteristics of lignocellulosic materials. In the region between 3000 and 3600  $\text{cm}^{-1}$ , the band at 3335  $\text{cm}^{-1}$  was associated with the stretching vibrations of hydroxyl groups (-OH) of water and polysaccharides [35]. The bands at 2915 and 2853  $\text{cm}^{-1}$ , were attributed to C-H stretching vibrations of C-H and  $\text{CH}_2$ , respectively, associated with cellulose and hemicellulose. The band at 1738  $\text{cm}^{-1}$  is associated with the vibration of the C=O in the ester group of hemicellulose or the ester bonds within the carboxylic groups in lignin [31], which removes dipole from the carbonyl and therefore its intensity is low. The band at 1600  $\text{cm}^{-1}$  has been associated with the bending of O-H in adsorbed water and also with polyphenols also reported in yerba mate by Ramirez Tapias, Monte, Peltzer and Salvay [36].

A weak band is observed at 1502  $\text{cm}^{-1}$ , which could be attributed to the C=C vibration of aromatic rings in the lignin structure, also found in the fiber of *Calamus tenuis* (Jati Bet) cane described by Kar and Saikia [31]. The three weak bands at 1422, 1322, and 1240  $\text{cm}^{-1}$ , were associated with  $\text{CH}_2$  bending in cellulose, C-O-C bending in hemicellulose, and C-O stretching of acetyl groups in lignin [5,31]. The main intense band with shoulders at 1031  $\text{cm}^{-1}$  corresponds to the vibration of pyranose rings and -CO-C glycosidic linkages between glucose from the cellulose structure [36]. A band observed in 607  $\text{cm}^{-1}$  may be associated with the bending of C-OH [31]. As expected, the FTIR spectrum of topinambur fiber shows hydroxyl groups that can interact with the hydroxyl groups of the starch matrix by forming hydrogen bonds, providing interfacial adhesion, and improving film properties.



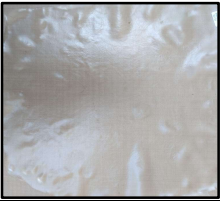
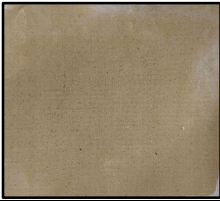



**Figure 3.** ATR: FTIR spectrum of topinambur fiber.

### 3.2. Characterization of Starch Films and Biocomposites

The effect of filler addition on starch film color parameters is shown in Table 2. Luminosity parameter (L) decreased significantly ( $p < 0.05$ ) with the increase of filler content while red-green ( $a^*$ ), yellow-blue ( $b^*$ ), and color difference ( $\Delta E$ ) parameters increased with the fiber aggregate. Chromaticity parameter  $b^*$ , exhibited the greatest change, indicating a predominantly yellowish ( $18 < b^* < 44$ ), and parameter  $a^*$  showed that were slightly reddish due to the positive values of  $a$  ( $0 < a^* < 5$ ) [35]. Visually, it was observed that the topinambur fiber was well dispersed throughout the starch matrix, with a brownish tone due to the phytochemicals such as the lignin content and a possible Maillard reaction [36], maintaining their transparency and homogeneity with no cracks (photographs insert in Table 2). Although, the use of bleaching treatments with NaOH solutions is a strategy to obtain a clear film [36], our interest was to avoid any extra chemical treatments to preserve the sustainability of the final material.

**Table 2.** Thickness, density and color parameters of cassava starch films with different fiber content.

Filler Content	0%	5%	10%
			
Thickness ( $\mu\text{m}$ )	$320 \pm 16^a$	$390 \pm 10^b$	$390 \pm 10^b$
Density ( $\text{g}/\text{cm}^3$ )	$1.44 \pm 0.04^a$	$1.55 \pm 0.05^b$	$1.51 \pm 0.02^b$
L (luminosity)	$90.0 \pm 0.4^c$	$70.8 \pm 0.8^b$	$60 \pm 2^a$
$a^*$ (red-green)	$0.19 \pm 0.05^a$	$2.9 \pm 0.6^b$	$7.7 \pm 0.5^c$
$b^*$ (yellow-blue)	$7.7 \pm 0.3^a$	$28 \pm 2^b$	$34.6 \pm 0.8^c$
$\Delta E$ (color difference)	$7.0 \pm 0.3^a$	$34.70 \pm 0.2^b$	$50.45 \pm 0.07^c$

**Note:** Reported values correspond to the mean  $\pm$  standard deviation. Different letters within the same line indicate significant differences ( $p < 0.05$ ).

The study of the UV light absorption capacity of biodegradable films is relevant to determine their possible applications for packaging as well as for agronomic applications such as mulching or potting. Thickness and film optical properties are shown in Table 3. Cassava starch film exhibited a thickness value around  $320 \mu\text{m}$  and as expected the incorporation of fiber led to a significant increase, with thickness proximate to  $390 \mu\text{m}$ . Density also increased with fiber incorporation, consistent with the higher density of lignocellulosic fibers compared to the polymer matrix. Reinforced films UV spectra showed a

characteristic peak at 250–300 nm (Figure 4), which can be associated with the phenolic components of lignin [19]. For the determination of the UV barrier capacity, the area under the curve in the UV region was calculated (200–400 nm), as it can be expected this parameter increased with topinambur fiber content of 0, 5, and 10%. Opacity was calculated from the spectra visible range (400–700 nm), showing a similar, although less pronounced trend.

Regarding agricultural applications, these properties are determining factors in the use of these materials for tunnel greenhouses, since UV-B radiation (280–320 nm) can have a negative impact, causing a decrease in photosynthesis and biomass production [35]. Besides, Ultraviolet adsorbents are added to agricultural films to prevent UV-induced degradation and extend its lifetime, which may also cause the accumulation of these additives in soils [37,38].

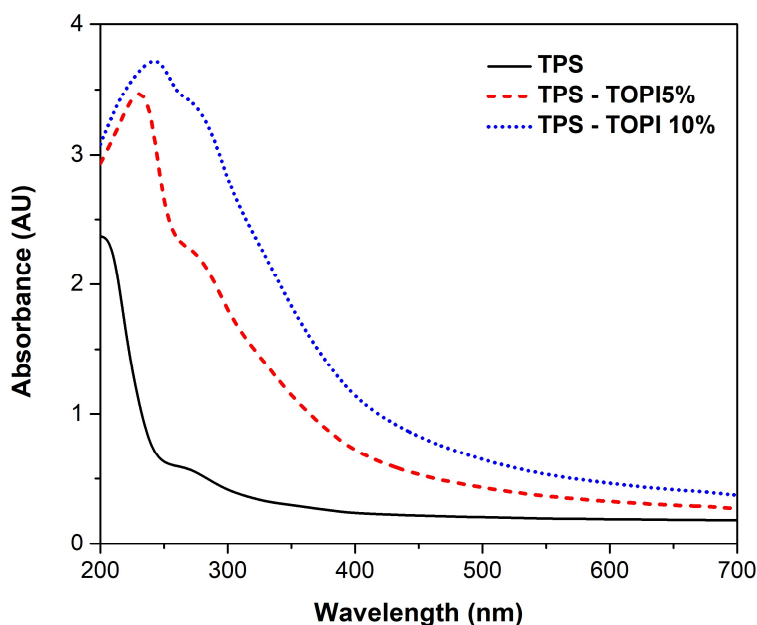


Figure 4. UV-vis spectra of TPS films with different fiber content.

Table 3. Optical properties of cassava starch films with different fiber content.

Filler Content	UV Barrier Property (AUxnm)	Opacity (AUxnm)
0%	126 ± 2 <sup>a</sup>	51 ± 9 <sup>a</sup>
5%	388 ± 3 <sup>b</sup>	119 ± 6 <sup>b</sup>
10%	533 ± 8 <sup>c</sup>	186 ± 5 <sup>c</sup>

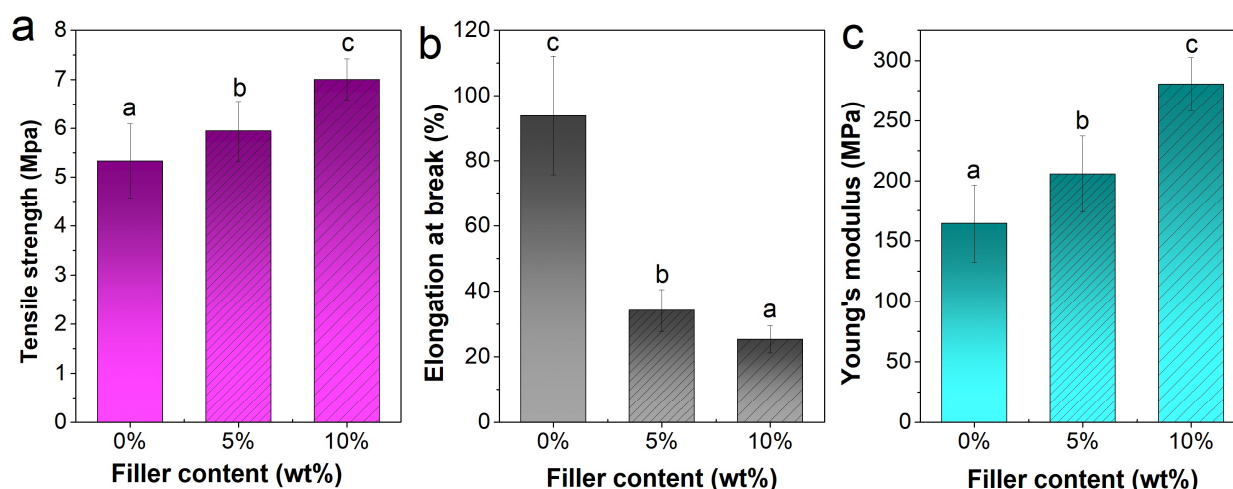
Note: Reported values correspond to the mean ± standard deviation. Different letters within the same column indicate significant differences ( $p < 0.05$ ).

This study investigated the effect of topinambur fiber content on the tensile strength, elongation at break, and elastic modulus of the starch biocomposites compared to the neat starch film; tested and stabilized at 50% relative humidity (RH) (Figure 5). The addition of filler slightly increased the tensile strength ( $p < 0.05$ ), (Figure 5a). The highest value was obtained with the addition of 10% topinambur fiber, showing the reinforcing effect of the topinambur fiber. According to other authors [14,39,40], this is due to strong interfacial interactions between the fiber and the TPS matrix, attributed mainly to hydrogen bond formation. This behavior could be related to a uniform dispersion of the fiber in the starch matrix without the formation of agglomerates. As a result, the stress is effectively transmitted from the starch matrix to the filler across the interface [41]. Besides, these results were supported by SEM images.

Similar results were obtained by Pongsuwan et al. [5] who investigated starch biocomposites reinforced with 5, 10, 15 and 20% banana inflorescence waste fibers and found an increase in tensile strength of more than 2 times with respect to the neat material, selecting the 10% content as optimal. Kaewtatip and Thongmee [42], showed similar results with the starch biocomposites reinforced with luffa fiber (*Luffa aegyptiaca*), with 5% increased tensile strength compared to neat starch and the maximum tensile strength was obtained with the addition of 10%, while on the contrary with the addition of 15 and 20%, the tensile strength decreased attributed to the agglomeration of excess of fiber. Therefore, with a fiber content of 5 and 10%, a reinforcing effect for the TPS matrix is achieved.



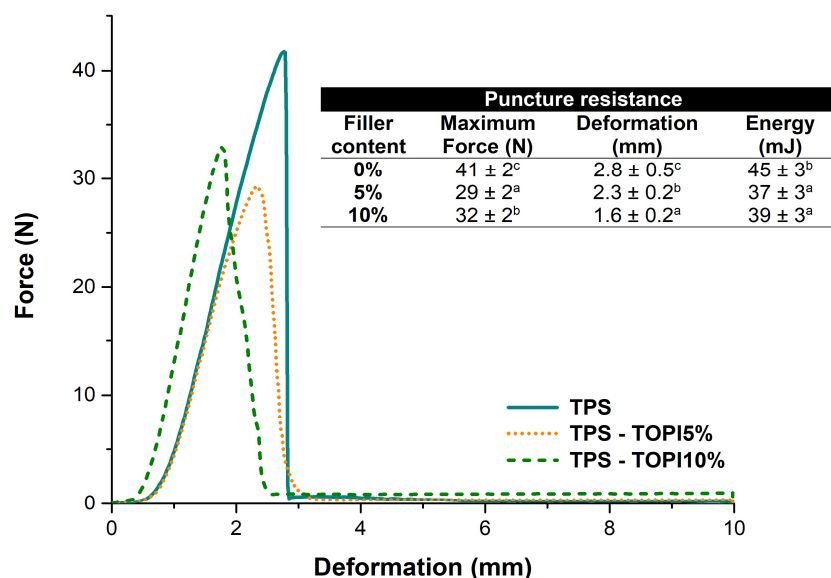
The elongation at break of the neat starch film decreased significantly ( $p < 0.05$ ) with the addition of both 5 and 10% of topinambur fiber (Figure 5b), due to the rigid nature of the fiber that limited the deformation and flexibility of the starch molecular chain. The increased rigidity was particularly notable with a loading of 10% topinambur fiber; this biocomposite exhibited the lowest elongation at break. As it could be observed the incorporation of the topinambur fiber as a reinforcing agent of the starch matrix led to stronger films, even with low filler incorporation. This result was evidenced by the increment in elastic modulus (Figure 5c), with significant differences ( $p < 0.05$ ) between the neat starch and the biocomposites. The 10% biocomposite was the one that had the highest value.



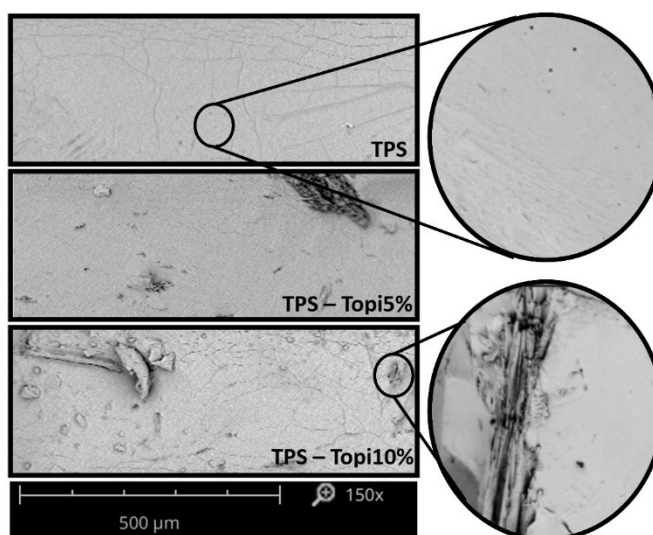
**Figure 5.** Tensile strength (a) elongation at break (b) and elastic modulus (c) of the neat starch and starch biocomposites. **Note:** different letters indicate significant differences between ( $p < 0.05$ ).

Materials for mulching used to cover soil typically need to be drilled for seedling implantation, as its main function is to maintain soil moisture and temperature and to prevent weed growth. Therefore, the resistance of the material to puncture is of interest for this application. The strength of starch biocomposites as indicated by the puncture force is shown in the table insert in Figure 6. The strength of the films and the energy required to perforate the material were significantly ( $p < 0.05$ ) lower for the films containing topinambur fiber, with the 5% fiber having the lowest strength and energy being the least puncture resistant formulation. These results are in agreement with those found by do Lago et al. [43] who studied the incorporation of wheat straw nanofibrils in a matrix of cassava starch and the elongation and puncture force decreased with the addition of the reinforcement. The reduction in puncture force values is attributed to the testing conditions, where the force is applied to the fiber membrane. In this sense, this force not only overcomes the friction between molecular chains, but also causes certain chains to break.

SEM micrographs of the cryo-fractured surfaces of films based on cassava starch (Figure 7), can be used to evaluate the microstructure and the distribution of the fiber in the matrix. The surface of neat starch film shows some traces of residual starch granules, but mostly a smooth and homogeneous surface. The addition of 5% of filler shows an irregular surface where filler particles are distributed along the entire starch matrix. In films with 10% filler, a greater number of particles is observed as expected. Interestingly, no gaps or holes are observed between the fillers and the TPS matrix, probably due to forming interactions between starch and cellulose/hemicellulose in the fiber (all carbohydrate compounds) [42]. This good interaction is consistent with the improved mechanical properties observed for the TPS-topinambur fiber biocomposites (Figure 5a).



**Figure 6.** Puncture resistance curves for one of ten replications of starch based films of control cassava 0% and reinforced with 5 and 10% topinambur fiber. Insert table: puncture resistance parameters of the material obtained. Mean values  $\pm$  standard deviation are presented; different letters in the same column indicate significant differences ( $p < 0.05$ ).

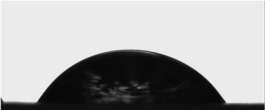
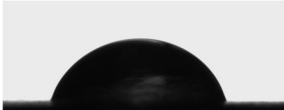
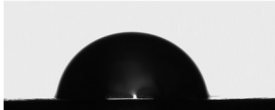


**Figure 7.** SEM micrographs of the cryofractured surface of cassava starch films without filler, 5% filler content and 10% filler content. Magnification used: 150 $\times$ .

Properties related to water are important for agriculture applications of starch-based bioplastics, as these are materials that are exposed to environmental conditions. In this study, the influence of topinambur fiber on water affinity was investigated by analyzing contact angle, moisture content, solubility, and water absorption (Table 4). The contact angle showed the hydrophilic nature of the neat starch film. The addition of topinambur fiber significantly ( $p < 0.05$ ) improved the hydrophobicity by increasing the contact angle with the fiber incorporation (pictures inserted in Table 4) due to the interaction between the fiber and starch molecules and the presence of inorganic and polyphenolic compounds in the structure of topinambur fiber [5].

The moisture of the films was significantly ( $p < 0.05$ ) affected by the fiber addition, as expected, an increase in the filler content resulted in a lower moisture content of the reinforced films, this reduction was consistent with the low moisture of topinambur fiber compared with the TPS matrix. This behavior can also explain the increase in contact angle by increasing topinambur fiber. Film solubility shows a similar trend since it also decreased with increasing fiber content, but the effect of reinforcement on solubility at room temperature was not significant ( $p > 0.05$ ).

**Table 4.** Water related parameters of cassava starch films with different fiber content.

Filler Content	0%	5%	10%
Contact angle (°)	 $57 \pm 4^a$	 $71 \pm 3^b$	 $79 \pm 4^c$
Moisture content (%)	$13.0 \pm 0.2^c$	$12.6 \pm 0.2^b$	$12.2 \pm 0.1^a$
Solubility (%)	$33.0 \pm 0.2^a$	$33.1 \pm 0.6^a$	$31 \pm 1^a$
Q (g water/100 g sample)	$0.270 \pm 0.006^a$	$0.260 \pm 0.007^a$	$0.250 \pm 0.006^a$
B (min)	$640 \pm 30^a$	$610 \pm 30^a$	$600 \pm 30^a$

**Note:** Reported values correspond to the mean  $\pm$  standard deviation. Different letters within the same line indicate significant differences ( $p < 0.05$ ).

The water uptake curves were adjusted to Elizalde, Pilosof and Bartholomai [27], the experimental data fit the proposed model satisfactorily ( $r^2 > 0.99$ ). The parameters Q and B were obtained (Table 4), reaching all the films a similar equilibrium value (Q), although the films reinforced with 10% topinambur fiber showed a lower initial water absorption rate (Q/B). For the biocomposite materials, water absorption decreased as the fiber content increased (Figure 8). Starch is more hydrophilic than fibers (cellulose, hemicellulose, and lignin) and the presence of topinambur fiber in the biocomposite increases the hydrophobicity. Furthermore, the strong adhesion between TPS and fiber creates a more complex pathway for water to penetrate, reducing the free volume of the starch matrix [42]. This can be contrasted with the report of Versino, Urriza and Garcia [44], who studied the water absorption at 100% RH of starch-based composite films reinforced with 1.5% cassava bagasse, where a higher equilibrium value (Q) ( $0.431 \pm 0.007$ ) and a shorter time (B) ( $17.3 \pm 3.5$ ) were found. In this case, observed differences are related to both formulation and processing conditions.

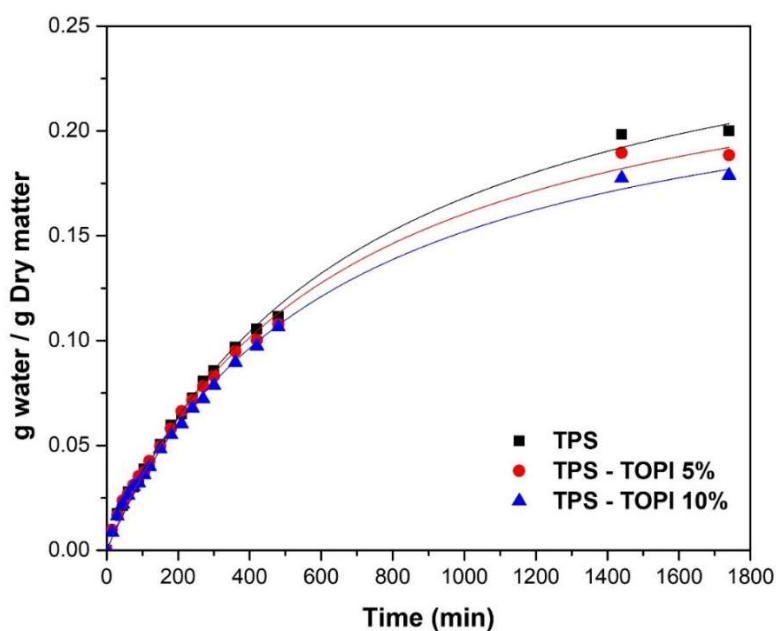


**Figure 8.** Predicted (solid lines) and experimental (single points) sorption curves at 100% RH of neat starch-based films and films reinforced with 5 and 10% topinambur fiber. The model fitting parameters Q and B are shown in the Table 4.

For comparative purposes, Table 5 summarizes the relevant properties of the materials developed in this study alongside those reported in literature for other TPS fiber-based composites. While comparing TPS materials is complex due to significant variations in final material properties depending on processing and base TPS composition (such as plasticizers presence and native starch source), it can be observed that the properties of our composites align with expected trends, reaffirming the effectiveness of natural fiber inclusion in TPS matrices. A noteworthy aspect of our composite is the improvement in hydrophobicity achieved through fiber inclusion, as demonstrated by the contact angle value.

**Table 5.** Comparison of mechanical, barrier, and other relevant properties of biocomposite reinforced films.

Biopolymer	Reinforcing Agent	Processing Technology	Mechanical Properties	Other Relevant Properties	References
Thermoplastic starch	-	-	E <sup>a</sup> = 125 MPa σ <sub>m</sub> <sup>b</sup> = 5.0–3.1 MPa ε <sub>B</sub> <sup>c</sup> = 9–31%	Optical transmission = 74% Water vapor barrier = 5.27 × 10 <sup>-10</sup> g/(m s Pa)	[15]
Pregelatinized cassava starch	Banana inflorescence waste fibers (5,10,15 and 20% wt)	Compression molding	σ <sub>m</sub> <sup>b</sup> = 0.2–0.51 MPa	Filler addition increased material rigidity especially with 10 wt%	[5]
Thermoplastic starch	Carbon ashes (0, 7, 14, and 21 %wt)	Melt mixing and compression molding	E <sup>a</sup> = 27.87–32.19 MPa σ <sub>m</sub> <sup>b</sup> = 2.27–2.65 MPa ε <sub>B</sub> <sup>c</sup> = 33–66%	Crystallinity degree = 12.7–22.2% Ashes decreased 70% the starch deterioration	[45]
Thermoplastic starch	Luffa ( <i>Luffa aegyptiaca</i> ) fiber (0–20% wt)	Compression molding	σ <sub>m</sub> <sup>b</sup> = 0.6–1.24 MPa ε <sub>B</sub> <sup>c</sup> = 35% with 10% fiber	Water absorption after 7 days of biocomposite with 20% wt was 14.3%	[42]
Thermoplastic starch	Agave fibers and henquen fibers (0, 10, 20 and 30%wt)	Extrusion and injection molding	E <sup>a</sup> = 128–454 MPa σ <sub>m</sub> <sup>b</sup> = 11–23 MPa ε <sub>B</sub> <sup>c</sup> = 10–463%	Fire retardant properties	[46]
Thermoplastic starch	Cassava and ahipa peel and bagasse (0.5 and 1.5 wt %)	Melt-mixing and compression molding	E <sup>a</sup> = 78.2–217.9 MPa σ <sub>m</sub> <sup>b</sup> = 2.6–5.5 MPa ε <sub>B</sub> <sup>c</sup> = 33.7–76.5%	Light and UV blocking capacity Water vapor barrier = 1.24–1.56 × 10 <sup>-10</sup> g/(m s Pa)	[47]
Cassava starch	Cassava bagasse (1.5% wt)	Casting	E <sup>a</sup> = 1247 ± 35 MPa σ <sub>m</sub> <sup>b</sup> = 14.73 ± 2.12 MPa ε <sub>B</sub> <sup>c</sup> = 5.81 ± 1.9%	Q <sup>d</sup> = 0.4308 ± 0.007 and B <sup>e</sup> = 1.35 ± 3.5 t <sub>50</sub> <sup>f</sup> = 33.18 days Water vapor barrier = 1.46 ± 0.07 × 10 <sup>-10</sup> g/(m s Pa)	[44]
Cassava starch	Wheat straw nanofibrils (30–50% wt)	Casting	E <sup>a</sup> = 566–585 MPa σ <sub>m</sub> <sup>b</sup> = 5.2–12.7 MPa ε <sub>B</sub> <sup>c</sup> = 84–57% (puncture test)	Contact angle = 43.45–68.6 ° Hue = 87.94–92.25 Water vapor barrier = 2.15–1.39 × 10 <sup>-10</sup> g/(m s Pa)	[43]
Thermoplastic cassava starch	Topinambur fiber (0–10% wt)	Extrusion and thermocompression	E <sup>a</sup> = MPa σ <sub>m</sub> <sup>b</sup> = 5.3–7.0 MPa ε <sub>B</sub> <sup>c</sup> = 94–25%	Contact angle = 57–79 ° Hue = 77.42–88.59 Q <sup>d</sup> = 0.25–0.27 B <sup>e</sup> = 595.49–635.77	This study

<sup>a</sup> Elastic modulus (E); <sup>b</sup> Maximum tensile strength (σ<sub>m</sub>); <sup>c</sup> Elongation at break (ε<sub>B</sub>); <sup>d</sup>Q water absorbed at equilibrium; <sup>e</sup>B time required to gain half of the equilibrium value; <sup>f</sup>t<sub>50</sub> mean time required for the degradation of 50% of the material, <sup>g</sup>WVP water vapor barrier.

The variations in the average percent biodegradation over time under soil conditions for the starch film samples and the MCC (microcrystalline cellulose) reference material are shown in Figure 9. Both MCC and starch films demonstrated a biodegradation percentage exceeding 55% within a 110 days' period. In this study, we conducted a biodegradation analysis in soil to emulate the effects on samples when subjected to real environmental conditions. While compost biodegradation is frequently assessed, it is crucial to acknowledge that the biodegradation rate in compost surpasses that in soil. This discrepancy is attributed to a greater abundance of microorganisms and favorable conditions, including heightened humidity and temperature, which facilitate accelerated biodegradation [48]. The results from the respirometric test indicate the aerobic biodegradation of both TPS films and those with the addition of topinambur fiber, as evidenced by mineralization or CO<sub>2</sub> generation. Composite films exhibited a similar behavior to TPS film and MCC, with no significant differences observed between the samples at the 110 day (Figure 9).

Thus, according to the results, it can be concluded that the addition of fiber as reinforcement in TPS films does not affect the biodegradability, since the trends of the film curves are similar to those of MCC. After 110 days, 100% of biodegradation in soil is not achieved. Therefore, the films could be suitable for use in short to medium term crops, reducing the environmental impacts associated with the plastic waste.

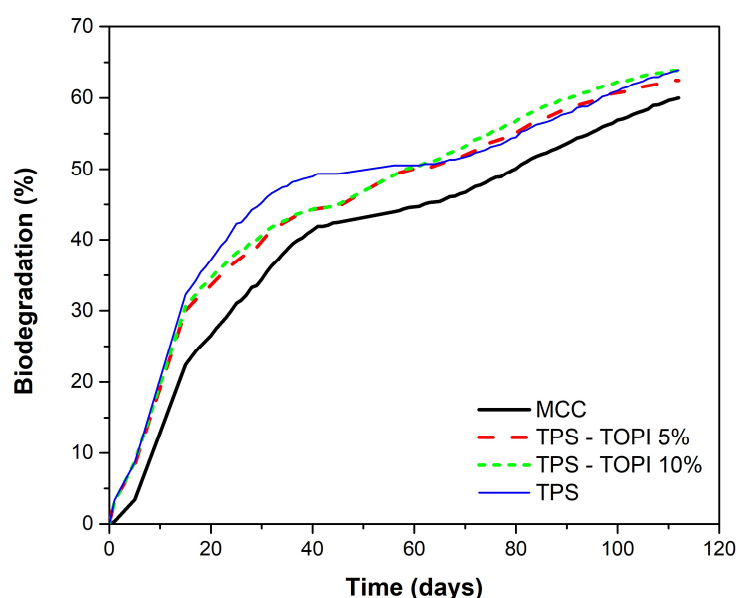


**Figure 9.** Biodegradation of TPS and TPS reinforced with 5 and 10% of topinambur fiber films under soil conditions (MCC biodegradation was included as reference).

Figure 10, shows the growth of tomato plants 15 days after planting in the control soil and in the residuals of the topi-5, topi-10 and TPS samples, respectively, after the biodegradation test. According to the results in Table 6, there were no significant differences ( $p > 0.05$ ) in the number of plants, in the maximum number of leaves for plant, in their height or fresh weight, between the control and the samples corresponding to the three treatments. As detailed in Table 6, the results suggest that the soil, having been in contact with the samples for 110 days, did not exhibit visible toxicity towards the plants. This non-toxic environment facilitated the successful germination and development of the tomato plants, being this fact significant agronomic applications.

**Table 6.** Ecotoxicity test of cassava starch based-films with different topinambur fiber content.

Fiber Content	Number of Plants	Nmax Leaves/Plant	Plant Height (cm)	Fresh Weight (g)
Control	8.5 ± 0.6 <sup>a</sup>	4.00 ± 0.01 <sup>a</sup>	8.15 ± 0.24 <sup>a</sup>	0.52 ± 0.04 <sup>a</sup>
0%	9.0 ± 1.4 <sup>a</sup>	4.00 ± 0.01 <sup>a</sup>	9.00 ± 0.28 <sup>a</sup>	0.55 ± 0.07 <sup>a</sup>
5%	9.5 ± 0.6 <sup>a</sup>	3.75 ± 0.01 <sup>a</sup>	8.65 ± 0.72 <sup>a</sup>	0.53 ± 0.08 <sup>a</sup>
10%	9.0 ± 0.8 <sup>a</sup>	4.00 ± 0.01 <sup>a</sup>	9.05 ± 1.68 <sup>a</sup>	0.53 ± 0.11 <sup>a</sup>

**Note:** Reported values correspond to the mean ± standard deviation. Different letters within the same column indicate significant differences ( $p < 0.05$ ).



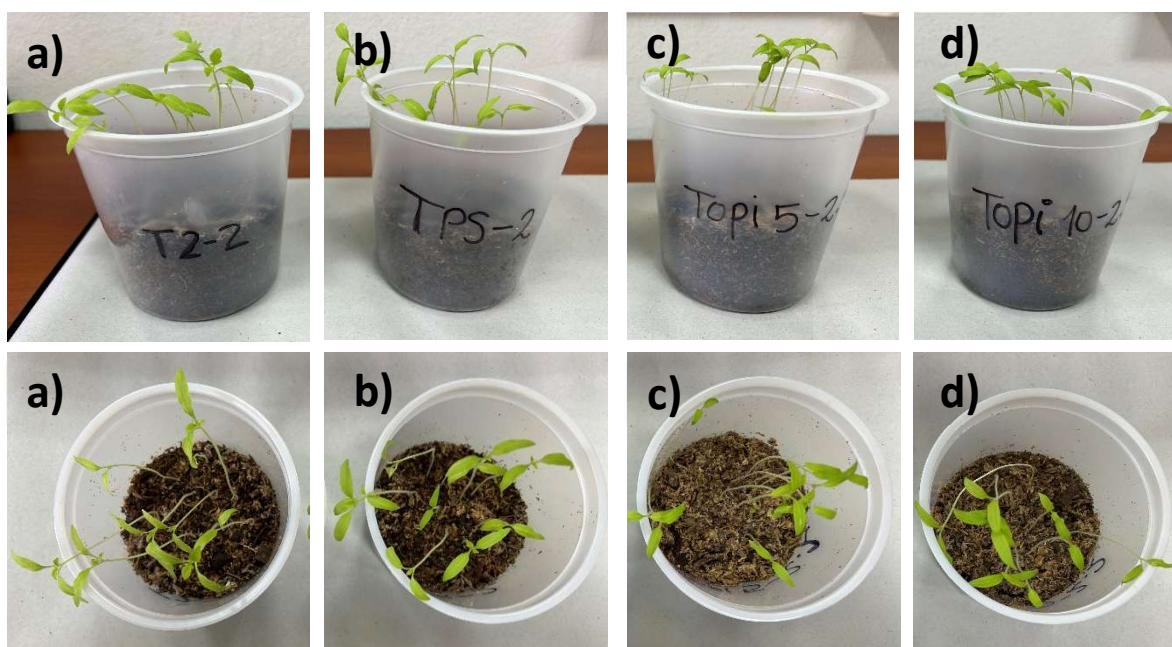


**Figure 10.** Photographs of tomato plant growth in residual soil during ecotoxicity test corresponding to the control (a) TOPI 5% (b) TOPI 10% (c) and TPS (d) films.

#### 4. Conclusions

This work showed the significant potential of natural fibers derived as a byproduct from topinambur production for developing TPS matrix biocomposites. These fibers, with around 40% cellulose, 14% hemicellulose and 24% lignin, improved the performance of starch-based bioplastic, in different approaches.

Reinforced films exhibited UV barrier capacity, which increases with filler content. Likewise, filler addition increased film opacity while decreased luminosity parameter. Topinambur fiber reinforced the polymeric matrix in both 5 and 10% filler, increasing the tensile strength and elastic modulus. SEM images showed some residual starch granules for TPS, and a homogeneous dispersion of the topinambur fiber throughout the matrix indicating a good interaction between both, which is consistent with the improved mechanical properties observed for the biocomposite materials.

Therefore, an integral approach to the aerial part of topinambur has been proposed providing added value to the remaining residue of topinambur crops. The properties of the biocomposite indicate that they could be adapted to the production of seedling pots or other agro ecological applications. These materials could be transplanted directly into soil while being degraded by soil microorganisms, without the release of pollutants, as an alternative to replace non-biodegradable synthetic materials, being an innovative additive within the circular economy premises.

#### Acknowledgements

The authors gratefully acknowledge Celina Bernal for the financial support provided by ANPCyT and Universidad de Buenos Aires of Argentina.

#### Author Contributions

The manuscript was written through contributions of all authors. All authors have given approval to the final version of the manuscript. The authors contributed equally.

#### Ethics Statement

Not applicable.

#### Informed Consent Statement

Not applicable.



## Funding

Authors acknowledge the financial support of Agencia Nacional de Promoción Científica y Tecnológica (ANPCyT, Projects: PICTA 2021-0095, PICT 2019-3843, PICT 2019-2827, and PICT 2017-2362) and Universidad de Buenos Aires (UBACYT 20020170100381BA) of Argentina.

## Declaration of Competing Interest

The authors declare that they have no known competing financial interests or personal relationships that could have appeared to influence the work reported in this paper.

## References

1. Wang S. International law-making process of combating plastic pollution: Status Quo, debates and prospects. *Mar. Policy* **2023**, *147*, 105376.
2. Walker TR, Fequet L. Current trends of unsustainable plastic production and micro(nano)plastic pollution. *TrAC—Trends Anal. Chem.* **2023**, *160*, 116984.
3. Flury M, Narayan R. Biodegradable plastic as an integral part of the solution to plastic waste pollution of the environment. *Curr. Opin. Green Sustain. Chem.* **2021**, *30*, 100490.
4. Ribba L, Lorenzo MC, Tupa M, Melaj M, Eisenberg P, Goyanes S. Processing and Properties of Starch-Based Thermoplastic Matrix for Green Composites. *Mater. Horizons Nat. Nanomater.* **2021**, 63–133, doi:10.1007/978-981-15-9643-8\_4/COVER.
5. Pongsuwan C, Boonsuk P, Sermwittayawong D, Aiemcharoen P, Mayakun J, Kaewtatip K. Banana inflorescence waste fiber: An effective filler for starch-based bioplastics. *Ind. Crops Prod.* **2022**, *180*, 114731.
6. Jiang J, Zhang X, Gao S, Li M, Hou H. Effects of adding methods and modification types of cellulose on the physicochemical properties of starch/PBAT blown films. *Int. J. Biol. Macromol.* **2022**, *223*, 1335–1343.
7. Raj T, Chandrasekhar K, Naresh Kumar A, Kim SH. Lignocellulosic biomass as renewable feedstock for biodegradable and recyclable plastics production: A sustainable approach. *Renew. Sustain. Energy Rev.* **2022**, *158*, 112130.
8. Amores-Monge V, Goyanes S, Ribba L, Lopretti M, Sandoval-Barrantes M, Camacho M, et al. Pineapple Agro-Industrial Biomass to Produce Biomedical Applications in a Circular Economy Context in Costa Rica. *Polymers* **2022**, *14*, 4864.
9. Raj H, Tripathi S, Bauri S, Mallick Choudhury A, Sekhar Mandal S, Maiti P. Green Composites Using Naturally Occurring Fibers: A Comprehensive Review. *Sustain. Polym. Energy* **2023**, *1*, 10010.
10. Luchese CL, Garrido T, Spada JC, Tessaro IC, de la Caba K. Development and characterization of cassava starch films incorporated with blueberry pomace. *Int. J. Biol. Macromol.* **2018**, *106*, 834–839.
11. Sifuentes-Nieves I, Yáñez Macías R, Neira Velázquez G, Velázquez G, Garcia Hernandez Z, Gonzalez Morones P, et al. Biobased sustainable materials made from starch and plasma/ultrasound modified Agave fibers: Structural and water barrier performance. *Int. J. Biol. Macromol.* **2021**, *193*, 2374–2381.
12. Armynah B, Anugrahwidya R, Tahir D. Composite cassava starch/chitosan/Pineapple Leaf Fiber (PALF)/Zinc Oxide (ZnO): Bioplastics with high mechanical properties and faster degradation in soil and seawater. *Int. J. Biol. Macromol.* **2022**, *213*, 814–823.
13. Mohammed AABA, Hasan Z, Borhana Omran AA, Elfaghi AM, Ali YH, Ilyas RA, Sapuan SM. Effect of sugar palm fibers on the properties of blended wheat starch/polyvinyl alcohol (PVA) -based biocomposite films. *J. Mater. Res. Technol.* **2023**, doi:10.1016/J.JMRT.2023.02.027.
14. Saepoo T, Sarak S, Mayakun J, Eksomtramage T, Kaewtatip K. Thermoplastic starch composite with oil palm mesocarp fiber waste and its application as biodegradable seeding pot. *Carbohydr. Polym.* **2023**, *299*, 120221.
15. Maraveas C. Production of Sustainable and Biodegradable Polymers from Agricultural Waste. *Polymers* **2020**, *12*, 1127.
16. Reborá C. Topinambur (*Helianthus tuberosus* L.): usos, cultivo y potencialidad en la región de Cuyo. *Hortic. Argent.* **2008**, *27*, 30–37.
17. Yang L, He QS, Corscadden K, Udenigwe CC. The prospects of Jerusalem artichoke in functional food ingredients and bioenergy production. *Biotechnol. Rep.* **2015**, *5*, 77–88.
18. Versino F, García MA. Cassava (*Manihot esculenta*) starch films reinforced with natural fibrous filler. *Ind. Crops Prod.* **2014**, *58*, 305–314.
19. Association of Official Analytical Chemists. Ash of flour. Direct method. AOAC (923.03). In *Official Methods of Analysis*; AOAC: Arlington, VA, USA, 1990.
20. Association of Official Analytical Chemists. Protein (crude) determination in animal feed: Copper catalyst Kjeldahl Method. AOAC (984.13). In *Official Methods of Analysis*; AOAC: Arlington, VA, USA, 1990.

21. Association of Official Analytical Chemists. Total dietary fibre in foods. Enzymatic-gravimetric method. AOAC (985.29). In *Official Methods of Analysis*; AOAC: Arlington, VA, USA, 1997.
22. Technical Association of the Pulp and Paper Industry. Acid-insoluble lignin in wood and pulp. T222 om-11. In *TAPPI Standards*; TAPPI Press: Atlanta, GA, USA, 2011.
23. Strack KN, García MA, Cabezas DM, Viña SZ, Dini C. Autoclaving and ultrasonication for reducing digestible starch in cassava pulp: modification of cell wall composition, sorption properties, and resistant starch content. *Int. J. Food Sci. Technol.* **2022**, *58*, 4911–4919.
24. Monroy Y, Seré P, Rivero S, García MA. Sustainable panels based on starch bioadhesives: An insight into structural and tribological performance. *Int. J. Biol. Macromol.* **2020**, *148*, 898–907.
25. American Society for Testing and Materials. Standard test method for haze and luminous transmittance of transparent plastics. ASTM D1003-00. In *Annual Book of ASTM*; ASTM International: Philadelphia, PE, USA, 2000.
26. American Society for Testing and Materials. Standard test method for tensile properties of thin plastic sheeting. ASTM 882-02. In *Annual Books of ASTM Standards: Designation*; ASTM International: Philadelphia, PE, USA, 1995; pp. 882–895.
27. Elizalde BE, Pilosof AMR, Bartholomai GB. Empirical model for water uptake and hydration rate of food powders by sorption and Baumann methods. *J. Food Sci.* **1996**, *61*, 407–409.
28. ISO17556, S. Plastics—Determination of the Ultimate Aerobic Biodegradability of Plastic Materials in Soil by Measuring the Oxygen Demand in a Respirometer or the Amount of Carbon Dioxide Evolved. ISO/TC, 61. 2019. Available online: <https://www.iso.org/standard/74993.html> (accessed on 23 October 2023)
29. Díaz-Díaz ED, Maldonado Haro ML, Patriarca A, Melaj M, Foresti ML, López-Córdoba A, et al. Assessment of the enhancement potential of salicylic acid on physicochemical, mechanical, barrier, and biodegradability features of potato starch films. *Food Packag. Shelf Life* **2023**, *38*, 101108.
30. OECD. *Terrestrial Plant Test: Seedling Emergence and Seedling Growth Test*; OECD-Organization for Economic Cooperation and Development: Paris, France, 2006.
31. Kar A, Saikia D. Characterization of new natural cellulosic fiber from *Calamus tenuis* (Jati Bet) cane as a potential reinforcement for polymer composites. *Heliyon* **2023**, *9*, e16491.
32. Fiore V, Scalici T, Valenza A. Characterization of a new natural fiber from *Arundo donax* L. as potential reinforcement of polymer composites. *Carbohydr. Polym.* **2014**, *106*, 77–83.
33. Almeida FA, Botelho EC, Melo FCL, Campos TMB, Thim GP. Influence of cassava starch content and sintering temperature on the alumina consolidation technique. *J. Eur. Ceram. Soc.* **2009**, *29*, 1587–1594.
34. Sriroth K, Santisopasri V, Petchalanuwat C, Kurotjanawong K, Piyachomkwan K, Oates CG. Cassava starch granule structure–function properties: influence of time and conditions at harvest on four cultivars of cassava starch. *Carbohydr. Polym.* **1999**, *38*, 161–170.
35. Tapias YAR, Monte MV, Di Peltzer MA, Salvay AG. Kombucha fermentation in yerba mate: Cellulose production, films formulation and its characterisation. *Carbohydr. Polym. Technol. Appl.* **2023**, *5*, 100310.
36. Ramírez Tapias YA, Di Monte MV, Peltzer MA, Salvay AG. Bacterial cellulose films production by Kombucha symbiotic community cultured on different herbal infusions. *Food Chem.* **2022**, *372*, 131346.
37. Carrasco-Ríos L. Efecto de la radiación ultravioleta-B en plantas. *Idesia (Arica)* **2009**, *27*, 59–76.
38. Li B, Liu Q, Yao Z, Ma Z, Li C. Mulch film: An overlooked diffuse source of organic ultraviolet absorbers in agricultural soil. *Environ. Pollut.* **2023**, *318*, 120935.
39. Chen J, Wang X, Long Z, Wang S, Zhang J, Wang L. Preparation and performance of thermoplastic starch and microcrystalline cellulose for packaging composites: Extrusion and hot pressing. *Int. J. Biol. Macromol.* **2020**, *165*, 2295–2302.
40. Fitch-Vargas PR, Camacho-Hernández IL, Rodríguez-González FJ, Martínez-Bustos F, Calderón-Castro A, Zazueta-Morales JdJ, et al. Effect of compounding and plastic processing methods on the development of bioplastics based on acetylated starch reinforced with sugarcane bagasse cellulose fibers. *Ind. Crops Prod.* **2023**, *192*, 116084.
41. Debnath B, Duarah P, Haldar D, Purkait MK. Improving the properties of corn starch films for application as packaging material via reinforcement with microcrystalline cellulose synthesized from elephant grass. *Food Packag. Shelf Life* **2022**, *34*, 100937.
42. Kaewtatip K, Thongmee J. Studies on the structure and properties of thermoplastic starch/luffa fiber composites. *Mater. Des.* **2012**, *40*, 314–318.
43. do Lago RC, de Oliveira ALM, de Amorim dos Santos A, Zitha EZM, Nunes Carvalho EE, Tonoli GHD, et al. Addition of wheat straw nanofibrils to improve the mechanical and barrier properties of cassava starch–based bionanocomposites. *Ind. Crops Prod.* **2021**, *170*, 113816.
44. Versino F, Urriza M, García MA. Eco-compatible cassava starch films for fertilizer controlled-release. *Int. J. Biol. Macromol.* **2019**, *134*, 302–307.
45. Stasi E, Giuri A, Ferrari F, Armenise V, Colella S, Listorti A, et al. Biodegradable Carbon-based Ashes/Maize Starch Composite Films for Agricultural Applications. *Polymers* **2020**, *12*, 524.

46. Sanchez-Olivares G, Rabe S, Pérez-Chávez R, Calderas F, Schartel B. Industrial-waste agave fibres in flame-retarded thermoplastic starch biocomposites. *Compos. Part B Eng.* **2019**, 107370, doi:10.1016/j.compositesb.2019.107370.
47. Versino F, López OV, García MA. Exploitation of by-products from cassava and ahipa starch extraction as filler of thermoplastic corn starch. *Compos. Part B Eng.* **2020**, 182, 107653.
48. Abe MM, Branciforti MC, Nallin Montagnolli R, Marin Morales MA, Jacobus AP, Brienzo M. Production and assessment of the biodegradation and ecotoxicity of xylan- and starch-based bioplastics. *Chemosphere* **2022**, 287, 132290.